

# Effect of Shearing on Crystallization Behavior of Poly(ethylene terephthalate)

HEE SOO MYUNG, WON JAE YOON, EUI SANG YOO, BYOUNG CHUL KIM, SEUNG SOON IM

Department of Textile Engineering, Hanyang University, Haengdang, Seongdong, Seoul 133-791, Korea

Received 23 January 2000; accepted 6 June 2000

**ABSTRACT:** The shear-induced crystallization behavior of PET was investigated by measuring the time-dependent storage modulus ( $G'$ ) and dynamic viscosity ( $\eta'$ ) with a parallel-plate rheometer at different temperatures and shear rate. The morphology of shear-induced crystallized PET was measured by DSC, X-ray, and polarizing optical microscopy. When a constant shear rate was added to the molten polymer, the shear stress increased with the time as a result of the orientation of molecular chains. The induction time of crystallization is decreased with frequency. Moreover, the rate of isothermal crystallization of PET was notably decreased with increasing temperature. The shape of spherulites is changed to ellipsoid in the direction of shear. In addition, aggregation of spherulites is increased with increasing frequency. Particularly, the row nucleation morphology could be observed under polarized light for  $\omega = 1$ . From the results of DSC, the melting point and enthalpy have a tendency to decrease slightly with increasing frequency. The crystallite size and perfectness decreased with frequency, which was confirmed with X-ray data. The unit length of the crystallographic unit cell of the PET increased and the  $(\bar{1} 0 3)$  plane peak increased with increasing frequency. © 2001 John Wiley & Sons, Inc. *J Appl Polym Sci* 80: 2640–2646, 2001

**Key words:** poly(ethylene terephthalate) (PET); rheology; shear-induced crystallization; crystallite

## INTRODUCTION

It is well recognized that the mechanical properties of plastic products are greatly affected by microstructure determined during the fabrication process. The microstructures are determined by the choice of processing conditions such as melting, solidifying, and shearing. In the fabrication processes the polymeric materials undergo complicated thermal and shear histories, which have a profound influence on the structure of the product. Many recent investigations have focused on

understanding the effect of shear history on the crystallization of crystalline polymers. Such studies have a practical importance because most of the polymer fabrication processes usually involve complex deformation histories. The flow stress is reported to accelerate the crystallization of crystalline polymers because the shear stress gives rise to the molecular orientation, reducing the entropy of the melt.<sup>1–6</sup> Thermodynamically, the reduced entropy raises the melting temperature, which results in increased supercooling.<sup>3,7</sup>

Several studies on PET were previously described in the literature; the elongational flow-induced crystallization behavior and memory effect of shear history of PET were investigated with rheometer and DSC.<sup>8–12</sup> However, the experiments of shear-induced crystallization of PET

Correspondence to: S. Im (E-mail: Imss007@email.hanyang.ac.kr)

*Journal of Applied Polymer Science*, Vol. 80, 2640–2646 (2001)  
© 2001 John Wiley & Sons, Inc.

on the rheological base did not seem to include X-ray data. Although there have been many results reported on X-ray data for the drawn PET films or fibers,<sup>13–17</sup> X-ray experiments on shear-induced crystallized PET have not been carried out. In this study, the shear-induced crystallization behavior of PET was investigated. In addition, the effect of shear history on the crystalline structure is also discussed in terms of thermal and morphological properties on the basis of X-ray data.

## EXPERIMENTAL

### Physical Properties

The material used in this study was poly(ethylene terephthalate) supplied by SK Chemicals (Korea). The polymer was predried in a vacuum oven at 120°C for 24 h. The inherent viscosity of 0.344 dL/g was determined in a mixture of trifluoroacetic acid and chloroform (1/3 v/v %) with a Ubbelohde viscometer at  $25 \pm 0.1^\circ\text{C}$ .

The apparatus used was the Advanced Rheometric Expansion System (ARES; Rheometric Scientifics) with the parallel-plate geometry. The plate diameter was 12.5 mm, the strain level was 5%, and the gap between the plates was 1 mm. The PET chips were heated to 300°C. The initial gap was set to a value equivalent to final gap plus 50  $\mu\text{m}$ . Excess sample was trimmed off. The value was reset to a final gap value of 1 mm and samples were relaxed for about 5 min at the temperature in a nitrogen atmosphere, after which they were cooled to be desired measurement temperature at a cooling rate of 20°C/min. A time-sweep experiment was performed on the molten polymer systems until the storage modulus reached a ceiling value (a value at level-off of the curve). After shearing, the sample was detached from the parallel plate for the DSC, X-ray diffractometer, and polarizing optical microscopy.

### Thermal Properties

Thermal analysis was carried out from 50 to 300°C at the heating rate of 10°C/min using a Perkin–Elmer DSC-7 (Perkin–Elmer, Foster City, CA) with nitrogen purge. The isothermal crystallization was fulfilled in two measurements. First, the samples were heated to 300°C at the rate of 200°C/min, held for about 5 min, then cooled to the desired measurement temperature

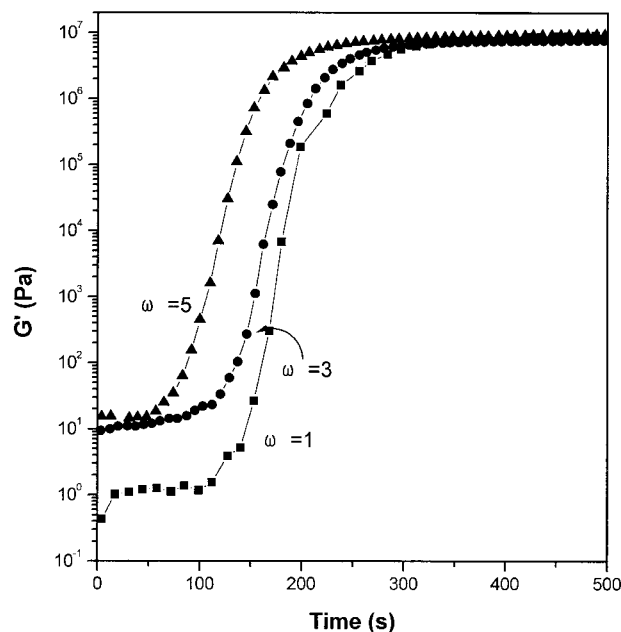


**Figure 1** Variation of  $G'$  with time for PET melt at 220°C at three different frequencies.

and crystallized at this temperature for the same time as with the ARES experiments. Second, PET chips were melted at 300°C between two glass slides for 5 min using the hot stage. They were very quickly moved to an oil bath and isothermally crystallized at 220, 230, and 240°C for 2, 4, and 10 h, respectively.

### Morphological Properties

Wide-angle X-ray diffraction patterns of the samples isothermally crystallized in the oil bath and the ARES tests were recorded on an X-ray diffractometer (Rigaku Denki) with Ni-filtered  $\text{CuK}\alpha$  radiation at 35 kV and 35 mA. Morphology of quiescent and shear-induced crystallized PET specimens was observed by polarized microscopy (Nikon HFX-IIA). The spherulite structure was observed by microtoming the specimens.

## RESULTS AND DISCUSSION

Figures 1 and 2 show the various results obtained for the  $G'$  (storage modulus) and  $\eta'$  (dynamic viscosity) versus time for three shear rates (1, 3, and 5 rad/s) at 220°C. The storage modulus value increased slowly during the early stage of experiments. The induction period is the stage when randomly entangled polymer chains transform to

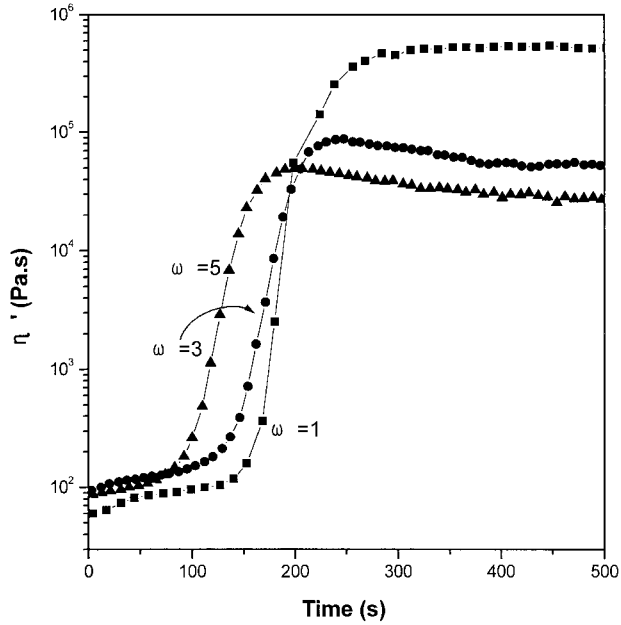


**Figure 2** Variation of  $\eta'$  with time for PET melt at 220°C at three different frequencies.

the regular aligned lattice. Because of topological obstruction of such entanglements, the polymer crystallization is extremely slow.<sup>18</sup> However, an abrupt increase of both parameters,  $G'$  and  $\eta'$ , follows in some minutes. This phenomenon can be inferred from the formation of crystallites, probably resulting from shear-induced crystallization. It may be, though, that the homogeneous PET melts change to a suspension system in which the crystallites disperse in the amorphous matrix.<sup>7,19–22</sup> The shear stress on the molten polymers results in two characteristic responses of the molecules, orientation and slippage. In view of macroscopic phenomena, the molecular orientation and slippage will correspond to elasticity and flow, respectively. An oriented polymer molecule has a lower entropy than that of a nonoriented one because of fewer possible conformations. Also, the free energy of the crystals equals that of the melt at the melting temperature. Therefore, for an oriented melt, the decrease in entropy may be considered to have increased the melting temperature and, therefore, supercooling.<sup>3</sup>

$$T_m = \frac{\Delta H_f}{\Delta S_f} = \frac{H_m - H_c}{S_m - S_c} \quad (1)$$

This is the reason that the induction time decreased with increasing frequency, as shown in

Figures 1 and 2. Figure 1 shows that the ceiling value of  $G'$  is the same, regardless of frequencies and temperatures when crystallization was finished. On the other hand, the ceiling value of  $\eta'$  is decreased by increasing the applied frequency, as shown in Figure 2. For example, a decrease in frequency from 3 to 1 rad/s led to an abrupt increase of viscosity. Such an abrupt increase of viscosity in the low-frequency range suggests the disappearance of zero-shear viscosity, which demonstrates the existence of a positive yield stress, indicating the system is heterogeneous.<sup>23</sup> In addition, the ceiling value of  $\eta'$  shows a gradual decrease with time after having reached a maximum as shown in Figure 2, which is more noticeable at the higher frequency. The gradual decrease of  $\eta'$  seems to result from the restructuring of the heterogeneous systems; that is, the viscosity is decreased with shearing because of destruction of the ordered crystallite particle structure. The destruction of the pseudostructure of crystallite particles is increased as shear rate is increased, as reflected in Figure 2.

Figure 3 shows the time-dependent rheological parameters at different crystallization temperatures and frequencies. As can be seen from these plots, both storage modulus and dynamic viscosity are very susceptible to structural changes in the fluid, and induction time is decreased with increasing temperature. This suggests that the number and growth rate of the nucleated crystallites is greater at 220°C than that at 240°C; that is, both nucleation density and growth rate of crystallites are diminished by raising the annealing temperature. This stands to reason because the maximum rate of the homogeneous crystallization of PET melts is observed in the vicinity of 190°C.<sup>24,25</sup>

The viscosity behavior of the PET melt with crystallization (Fig. 3) may be accounted for by adopting the Mooney equation in a qualitative manner<sup>26</sup>:

$$\ln\left(\frac{\eta}{\eta_1}\right) = \frac{K_B \Phi_2}{1 - (\Phi_2/\Phi_m)} \quad (2)$$

$$\Phi_m = \frac{\text{True volume of filler}}{\text{apparent volume occupied by the filler}} \quad (3)$$

where  $\eta$  is the viscosity of the suspension,  $\eta_1$  is the viscosity of the suspending medium,  $\Phi_2$  is the volume fraction of the filler,  $\Phi_m$  is the maximum

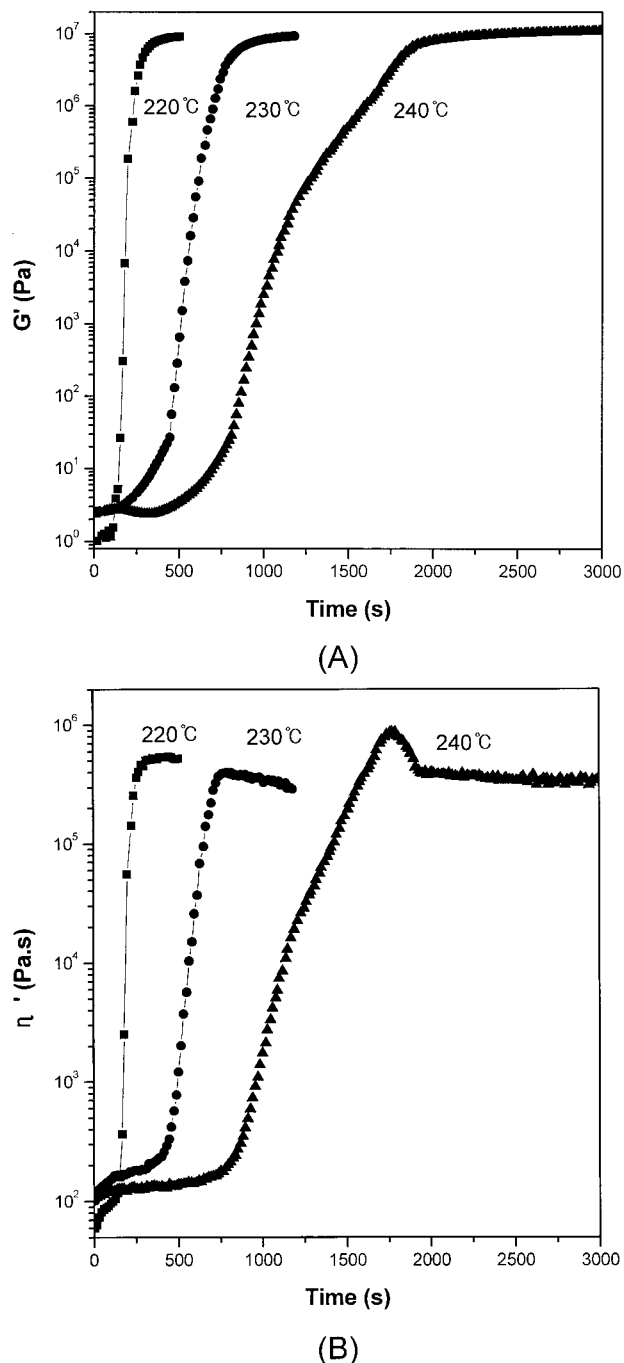


**Figure 3** Variation of  $G'$  (A) and  $\eta'$  (B) for PET melt at 3 rad/s at three different temperatures.

volume fraction that the filler can have, and  $K_E$  is the Einstein coefficient, whose value is known to be 2.5 for the dispersed spherical filler.

Referring to the Mooney equation, the crystallization patterns of PET melts at both 220 and 240°C are distinctively different. The Mooney equation predicts that the degree of increase in

suspension viscosity with increasing  $\Phi_2$  is greatly increased if the spheres form aggregates because the aggregation of spheres (spherulitic crystallites or crystals in this study) increases the apparent filler volume fraction. On this assumption, it may be suggested that an application of higher shear rate during isothermal crystallization tends to increase the heterogeneous crystallization characteristics. Hence, the higher nucleation density and higher growth rate of the nucleated crystallites are obtained at higher frequency. Moreover, this can be confirmed, as shown in Figure 4, which indicates that nucleation becomes increasingly profuse and the size of spherulites decreases with increasing frequency. In Figure 4(b) row nucleation is observed for  $\omega = 1$ , which is evidence of the effect of shearing and also that the shape of spherulites by shearing is elliptical.<sup>12</sup> When frequency increases, aggregation of spherulites is often observed and the size of spherulites decreases. Indeed, in the photograph of the PET sample crystallized for  $\omega = 5$ , the spherulites filled in the whole range because of the higher nucleation density and higher growth rate of the nucleated crystallites.

The melt endotherms of quiescently and shear-induced crystallized PET are shown in Figure 5. In Figure 5,  $\omega = 0$  rad/s indicates quiescent crystallization: (a) indicates that the PET sample was crystallized at 240°C for the same time as that required in the ARES experiments, and (b) expresses the PET sample crystallized in an oil bath at the same temperature as in (a) for a time long enough to fully crystallize. Because the holding time at crystallization temperature in (a) is much shorter than that in (b), an exothermic peak of crystallization during the DSC heating scan is observed in the thermogram (a) at around 155°C. When the shear stress was applied, the induction time of crystallization decreased and the possibility of nuclei formation increased as a result of molecular orientation. These results make the overall bulk crystallization rate more speedy, resulting in the disappearance of the exothermic peak in the upper three peaks of Figure 5.

In general, for the sheared melt the ensuing reduction in entropy increases  $T_m$ , as shown in eq. (1). As frequency increased, induction time of crystallization decreased as a result of molecular orientation, which indicates a reduction of  $\Delta S_f$ . In addition, the size and perfectness of crystallites decreased with increasing frequency (this is discussed later in detail), which is the reason that  $\Delta H_f$  decreased with frequency, even though the

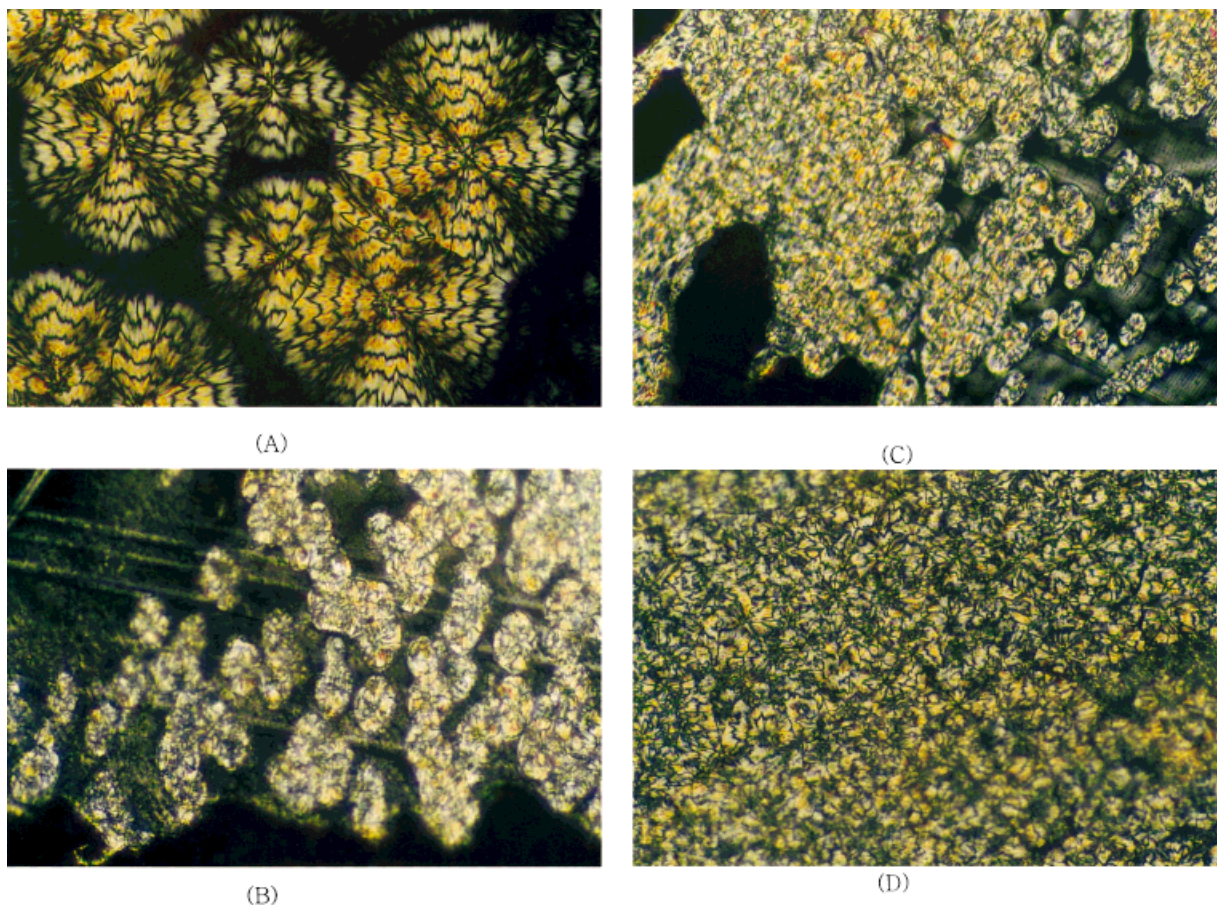


**Figure 4** Polarizing optical micrographs of PET crystallized at 240°C at the following frequencies: (A)  $\omega = 0$ , (B)  $\omega = 1$ , (C)  $\omega = 3$ , and (D)  $\omega = 5$ . [Color figure can be viewed in the online issue, which is available at [www.interscience.wiley.com](http://www.interscience.wiley.com).]

amount of reduction was scarcely noticeable. In the previous work,<sup>27</sup> the sheared molecular chain of PEN was better oriented than that of PET because of its rigid backbone, and it was supposed that the reduction of  $\Delta S_f$  might be greater than that of  $\Delta H_f$ . Consequently,  $T_m$  increased with increasing frequency. On the other hand, in the case of PET, which has the more flexible backbone, it may be thought that the reduction of  $\Delta S_f$  was similar to that of  $\Delta H_f$ ; hence, the melting point of PET was not changed with frequency.

Figure 6 presents WAXD patterns of PET specimens with shear-induced crystallization at 240°C at several frequencies. For the separation of peaks, we used the method of Hindeleh and Johnson,<sup>28</sup> which is the only procedure based on a reliable mathematical method for resolution of overlapping peaks and separation of amorphous scatter. This method has been successfully applied to the X-ray investigations of cellulose,<sup>29–31</sup> polyamide, and poly(ethylene terephthalate) fi-

bers.<sup>32</sup> In this method, an experimental X-ray diffraction pattern is approximated by the theoretical function

$$Y_c = \sum_{i=1}^k Q_i + B \quad (4)$$

where  $k$  is the number of crystalline peaks.  $Q$  is expressed as either a Gaussian or a Cauchy function, or as a combination of both.  $B$  is a background function, which can be expressed as a polynomial:

$$B = a + bx + xd^2 + dx^3 \quad (5)$$

where  $x$  is the scattering angle  $2\theta$ .

$$Q_i = f_i A_i \exp \left\{ -\ln 2 \left[ \frac{2(x - P_i)}{W_i} \right] \right\} + \frac{(1 - f_i) A_i}{1 + [2(x - P_i)/W_i]^2} \quad (6)$$

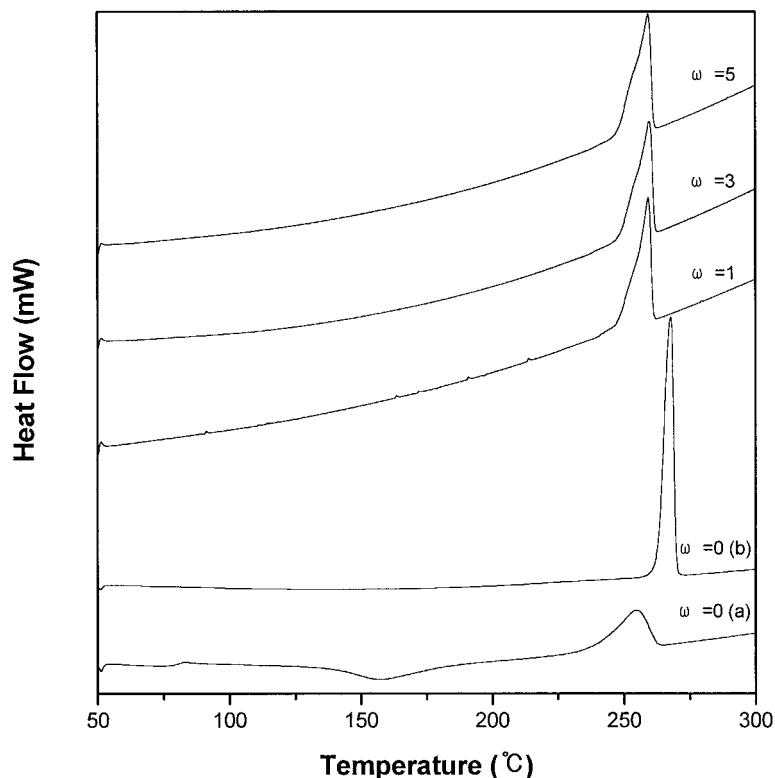


**Figure 5** DSC thermograms of PET isothermally crystallized at 240°C at various frequencies.

Each peak is represented by four parameters:  $A_i$ , the peak width at half-height  $W_i$ , the peak angular position  $P_i$ , and the profile function parameter

$f_i$  ( $f_i = 0$  for a Cauchy function,  $f_i = 1$  for a Gaussian function, and can be any fraction for combined functions). If necessary, other functions could be used in place of  $Q_i$  and  $B$ . All the parameters are found by minimization of the function

$$S = \sum_{i=1}^n (Y_{ci} - Y_{ei})^2 \quad (7)$$

where  $Y_{ci}$  and  $Y_{ei}$  are the calculated and experimental X-ray scattering intensities, respectively, and  $n$  is the number of intensity data. The minimization procedure is completed at a value of  $S$ , given by

$$S = r^2 \sum_{i=1}^n (Y_{ci})^2 \quad (8)$$

where  $r$  is the relative experimental error. As a result one can resolve multiple peak data into individual crystalline peaks, an amorphous region, and the half-width. The reciprocal of the half-height broadening is used as a reliable parameter to evaluate both size and perfectness of the crystal-

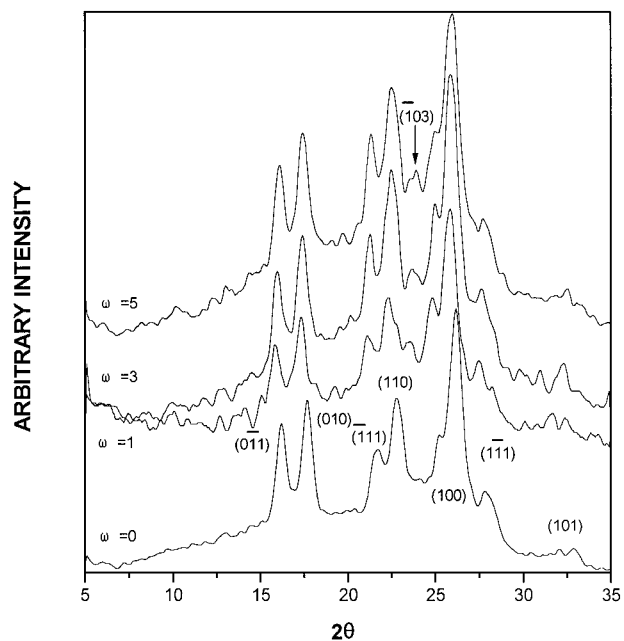


**Figure 6** WAXD patterns of PET isothermally crystallized at 240°C at various frequencies.

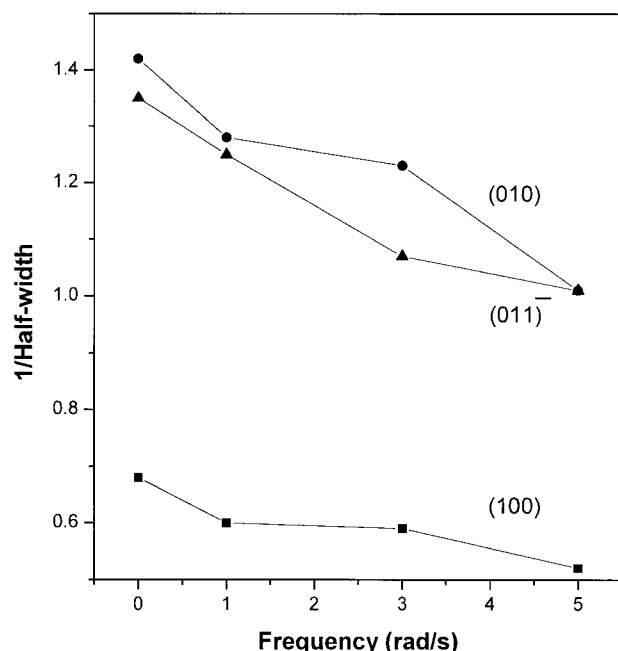


**Figure 7** The variation of mean crystallite size of PET isothermally crystallized at 240°C with frequency.

lites.<sup>33,34</sup> It is possible in this way to obtain the crystallites' size and perfectness from peak separation and the reciprocal of the half-width. Figure 7 presents the variation of the value of the reciprocal of the half-width with frequency. In Figure 7, the crystallites' size and perfectness of (0 1 1), (0 1 0), and (1 0 0) planes, which correspond to 25.9, 17.5, and 16.3°, respectively, have a tendency to decrease with increasing frequency, which is evidence of the reduction of  $\Delta H_f$  (in Fig. 5). In Figure 6, the (1 0 3) plane peak appears at around 24°, for  $\omega = 0$ , and keeps growing with increasing frequency. In addition, all diffraction peaks of Figure 6 shift to a lower angle when frequency is increased. This suggests that the unit length of the crystallographic unit cell of the PET changes slightly when crystallites grow under shear condition. The length increased with increasing frequency at every crystallization temperature. This deformation might be the result of the shear stress affecting the crystallites during or after crystalline formation. It could be suggested that the unit length deformation negatively affects the amount of  $\Delta H_f$ , like the value of 1/half-width.

This work was supported by grant No. 1999-2-301-006-5 from the Basic Research program of the Korea Science & Engineering Foundation.

## REFERENCES

- Hill, M. J.; Keller, A. *J Macromol Sci Phys* 1969, B3, 153.

- Andrews, E. H. *J Polym Sci* 1966, A2, 663.
- Haas, T. W.; Maxwell, B. *Polym Eng Sci* 1969, 9, 226.
- Pennings, A. J.; van der Mark, J. M. A. A.; Booj, H. C. *Kolloid Z Z Polym* 1970, 236, 99.
- Mackley, M. R.; Keller, A. *Polymer* 1973, 14, 16.
- Peterlin, A. *Polym Eng Sci* 1976, 16, 126.
- Kobayashi, K.; Nagasawa, T. *J Macromol Sci Phys* 1970, B4, 331.
- Kubo, H.; Sato, H.; Okamoto, M.; Kotaka, T. *Polymer* 1998, 39, 501.
- Okamoto, M.; Kubo, H.; Kotaka, T. *Polymer* 1998, 39, 3135.
- Kubo, H.; Okamoto, M.; Kotaka, T. *Polymer* 1998, 39, 4827.
- Okamoto, M.; Kubo, H.; Kotaka, T. In *Proceedings of the 13th Annual Meeting of the Polymer Processing Society (PPS-13)*, New York, 1997, Abstract No. 8-C.
- Kim, S. P.; Kim, S. C. *Polym Eng Sci* 1993, 33, 83.
- Hevel, H. H.; Huisman, R. *J Appl Polym Sci* 1978, 22, 2229.
- Fu, Y.; Busing, W. R.; Jin, Y.; Affholter, K. A.; Wunderlich, B. *Macromolecules* 1993, 26, 2187.
- Goschel, U.; Dentscher, K.; Abetz, V. *Polymer* 1996, 37, 1.
- Ajji, A.; Guevremont, J.; Cole, K. C.; Dumoulin, M. M. *Polymer* 1996, 37, 3707.
- Mahomdrasingam, A.; Martin, C.; Fuller, W.; Blundell, D. J. *Polymer* 1999, 40, 5553.
- Imai, M.; Kaji, K.; Kanaya, T.; Sakai, Y. *Phys Rev* 1995, B52, 12696.
- Titomanlio, G.; Brucato, V. Presented at the 10th Annual Conference of the Plastics Processing Society, Akron, OH, 1965; Paper 93.
- Eder, G.; Janeschitz-Kriehl, H.; Liedauer, S. *Prog Polym Sci* 1989, 15, 629.
- Wolkowicz, M. D. *J Polym Sci Polym Symp* 1978, 63, 365.
- Kim, J. G.; Park, H. J.; Lee, J. W. *Korean J Rheol* 1997, 4, 174.
- Pierre, J. C.; De Kee, D. C. R.; Chhabra, R. P. *Rheology of Polymeric Systems*; Hanser: New York, 1997.
- Cobbs, W. H.; Burton, R. L. *J Polym Sci* 1953, 10, 275.
- Morgan, L. B., et al. *Philos Trans R Soc London Ser A* 1954, 247, 1.
- Lawrence, E. N. *Polymer Rheology*; Marcel Dekker: New York, 1977.
- Yoon, W. J.; Myoung, H. S.; Kim, B. C.; Im, S. S. *Polymer* 2000, 41, 4933.
- Hindeleh, A. M.; Johnson, D. J. *J Phys* 1971, 4, 259.
- Hindeleh, A. M.; Johnson, D. J. *Polymer* 1972, 13, 27.
- Hindeleh, A. M.; Johnson, D. J. *Polymer* 1972, 13, 423.
- Hindeleh, A. M.; Johnson, D. J. *Polymer* 1974, 15, 697.
- Hindeleh, A. M.; Johnson, D. J. *Polymer* 1978, 19, 27.
- Vittoria, V. *J Macromol Sci Phys* 1989, B28, 489.
- Yoo, E. S.; Im, S. S. *Macromol Symp* 1997, 118, 739.